HOMOGENEOUS PRECIPITATION OF SILICEOUS MCM-41 AND BIMODAL SILICA

Jiri RATHOUSKY[a1], Marketa ZUKALOVA[a], Arnost ZUKAL[a2] and Jiri HAD[b]

[a] *J. Heyrovsky Institute of Physical Chemistry, Academy of Sciences of the Czech Republic, 182 23 Prague 8, Czech Republic; e-mail: [1] rathous@jh-inst.cas.cz, [2] zukal@jh-inst.cas.cz*

[b] *Central Laboratories, Prague Institute of Chemical Technology, 166 28 Prague 6, Czech Republic; e-mail: jiri.had@vscht.cz*

Received May 5, 1998
Accepted June 12, 1998

A new procedure for synthesis of MCM-41 siliceous molecular sieves with regular morphologies and bimodal mesoporous silica was developed. It is based on the precipitation from an isotropic reaction mixture. The decrease in pH, which causes the formation of solid particles, is achieved by the hydrolysis of ethyl acetate. The procedure is excellently reproducible and enables to obtain not only siliceous MCM-41 with the highest degree of pore ordering and phase purity but also a material of a new type, *viz.* bimodal silica containing both the MCM-41 mesopore system and the system of larger mesopores whose size ranges from 15 to 25 nm.

Key words: Siliceous MCM-41 mesoporous molecular sieves; Bimodal mesoporous silica; Homogeneous precipitation; Morphology control; Porous materials synthesis.

In 1992 the synthesis of a new family of mesoporous molecular sieves designated as M41S was reported[1,2]. MCM-41, one member of this family, has uniform cylindrical pores in hexagonal arrangement and is produced using rod-like micelles of cationic surfactant molecules as a template. The pore size of MCM-41 can be varied from 2 to about 10 nm. Two reviews of the extensive literature on M41S materials have been published in recent years[3,4].

Recently we have published a study dealing with the optimization of a synthesis route for the preparation of MCM-41 mesoporous molecular sieves from colloidal silica[5]. While this procedure enabled obtaining material with a high degree of ordering and phase purity, its particle shape was irregular with a very broad particle size distribution ranging from 0.5 to 5 μm.

In order to obtain highly-ordered mesoporous molecular sieves with regular and adjustable particle shape and size, a different synthesis strategy should be adopted. The precipitation in an homogeneous environment seems to be a promising procedure[6–8]. Therefore the present communication deals with a synthesis route based on the precipitation of siliceous mesoporous materials from an isotropic reaction mixture.

EXPERIMENTAL

Synthesis Field

The reaction mixture used consists of the silica source (sodium metasilicate, Na_2SiO_3), surfactant (cetyltrimethylammonium bromide, CTABr) and water, to which ethyl acetate (EtAc) is subsequently added. Due to the hydrolysis of EtAc a decrease in pH occurs, which causes the formation of solid particles. Sodium metasilicate was chosen as the silica source because of the necessity of ensuring the isotropy of the reaction mixture. For this reason, other often used sources, such as colloidal, fumed or fused silicas, cannot be used. The use of water glass (sodium silicates having $SiO_2 : Na_2O$ molar ratios 1.6–3.9) was found to be less suitable because it is a mixture of different oligomeric silicate anions.

The composition of the reaction mixtures and coding of samples prepared are summarized in Table I. Figure 1 shows the synthesis field in the form of a triangular diagram. Samples, which are prepared with the same molar ratio of $Na_2SiO_3 : CTABr : H_2O$, differing only in the amount of EtAc in the reaction mixture (given in Table I by the molar ratio $EtAc : Na_2SiO_3$), are always represented by the same points. As the solubility of CTABr in water does not exceed 0.5 mole % at 20 °C, the points in the triangular diagram virtually cover the whole region of possible concentrations.

Acetic acid, which is formed in the reaction mixture due to the hydrolysis of ethyl acetate, is consumed by the reaction with Na_2SiO_3. The formed ≡Si–OH groups are then transformed to ≡Si–O–Si≡ *via* the condensation reaction. The required molar ratio $EtAc : Na_2SiO_3$ was assessed on the basis of a known content of surfactant in as-synthesized MCM-41 materials prepared using cetyltrimethylammonium chloride or bromide. This content equals 45 wt.% as determined by thermogravimetric analysis[9,10]. The degree of crosslinking of the silica walls in these materials can be described by means of the "Q^n notation" (ref.[11]). In this notation, Q stands for a silicon atom bonded to four oxygen atoms forming a SiO_4 tetrahedron. The superscript *n* indicates the connectivity, *i.e.* the number of other Q units attached to the unit in question and the central silicon atom is written in bold. The SiO_4 tetrahedron is 4-connected and the remaining (4 – *n*) units linked to it are often hydroxyl groups. Thus, Q^4 stands for three-dimensionally cross-linked $\mathbf{Si}(OSi)_4$ units, Q^3 for $\mathbf{Si}(OSi)_3(OH)$ units and Q^2 for $\mathbf{Si}(OSi)_2(OH)_2$ units. The percentage of Q^n species is determined by the ^{29}Si MAS NMR spectroscopy. We have found[1] that $Q^2 \approx 6\%$, $Q^3 \approx 40\%$ and $Q^4 \approx 54\%$. Consequently, 1 g of an as-synthesized sample consists of ≈1.6 mmol of $CTMA^+$ and ≈8.6 mmol of Q^2, Q^3 and Q^4 species. To transform 8.6 mmol of Na_2SiO_3, necessary for the formation of 1 g of as-synthesized material, to silicic acid, 17.2 mmol of acetic acid are required. As 1.6 mmol of $\equiv Si–O^-$ groups serve as counter-

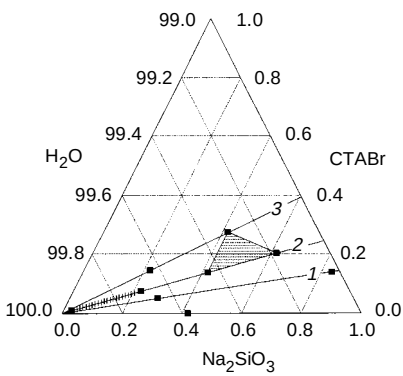

FIG. 1
Synthesis field diagram of silica structures established by XRD and nitrogen adsorption measurements (reactant concentrations given in mole %). The vertically and horizontally hatched areas depict the range of reactant concentrations where the pure MCM-41 phase and bimodal silicas are formed, respectively. Molar ratios of CTABr : $Na_2SO_3 \approx 0.17$ (*1*), 0.33 (*2*), 0.67 (*3*), see Table I

ions for $CTMA^+$, the actual consumption of acetic acid is decreased by 1.6 mmol. Thus the assessed molar ratio of EtAc : Na_2SiO_3 equals 1.8.

Although this calculation was carried out under the assumption of complete hydrolysis of EtAc, which cannot be fully true, experimental verification has proved that the calculated molar ratio is optimum for the synthesis of MCM-41 molecular sieves. While at the molar ratio EtAc : Na_2SiO_3 smaller than 1.8, the transformation of Na_2SiO_3 to solid product was incomplete, at larger values, a new type of mesoporous silica was obtained.

Synthesis

The reaction mixture was prepared directly in an autoclavable polypropylene bottle. 0–19.6 g of CTABr (Aldrich) followed by 10 g of solid Na_2SiO_3 (Aldrich) were dissolved in 350–667 ml of distilled water, resulting in a clear solution. Afterwards 14.3–25.5 ml of EtAc (Aldrich) was quickly added under stirring. After 1 min the stirring was stopped and the mixture was allowed to stand at ambient temperature for 5 h. After 5–10 min, a precipitate began to form. Then the reaction mixture was kept at 90 °C for 50 h in a heating box. During the ageing, organic vapour was allowed to evaporate through leaks in the cap of the bottle.

TABLE I
Composition of the reaction mixture and percentage of the MCM-41 structure in the synthesized silica

Silica	Na_2SiO_3 mole %	CTABr mole %	H_2O mole %	EtAc : Na_2SiO_3 mol/mol	CTABr : Na_2SiO_3 mol/mol	MCM-41 %
1B	0.413	0	99.587	3.2	0	0
2A	0.287	0.051	99.662	1.8	0.178	80
2B	0.287	0.051	99.662	3.2	0.178	40
3A	0.840	0.138	99.022	1.8	0.164	48
3B	0.840	0.138	99.022	3.2	0.164	26
4A	0.029	0.010	99.961	1.8	0.345	100
5A	0.227	0.076	99.697	1.8	0.335	91
5A-S	0.227	0.076	99.697	1.8	0.335	83
6A	0.419	0.140	99.441	1.8	0.334	66
7A	0.618	0.202	99.180	1.8	0.327	66
5B	0.227	0.076	99.697	3.2	0.335	48
6B	0.419	0.140	99.441	3.2	0.334	38
7B	0.618	0.202	99.180	3.2	0.327	27
8A	0.215	0.144	99.641	1.8	0.670	56
8B	0.215	0.144	99.641	3.2	0.670	39
9A	0.413	0.277	99.310	1.8	9.671	72
9B	0.413	0.277	99.310	3.2	0.671	36
9B-S	0.413	0.277	99.310	3.2	0.671	47

The most dilute reaction mixture containing 5 250 ml of water (sample 4A) was prepared in a glass vessel. After the precipitation with EtAc and prolonged ageing at ambient temperature for 50 h, MCM-41 particles sedimented. The clear solution over the precipitate was removed. Then the suspension of the solid product in the mother liquor was transferred into a polypropylene bottle and aged at 90 °C for 50 h.

The resulting solid was recovered by filtration of the still warm reaction mixture, extensively washed with distilled water and ethanol, and dried at ambient temperature. The template was removed by calcination at 600 °C for 20 h in flowing air.

The reproducibility of the synthesis procedure was checked using samples 5A and 9B characterized by a well-defined porous structure and regular morphology (see below). Their preparation was repeated with the starting amount of Na_2SiO_3 being varied from 5 to 25 g. With these samples, the influence of stirring on the properties of the solid product was also investigated. After the addition of EtAc, stirring was not stopped and the reaction mixture was stirred at ambient temperature for 5h. The samples prepared in this way are denoted as 5A-S and 9B-S (Table I).

Characterization

Powder X-ray diffraction data were obtained on a Seifert 3000 P diffractometer in the Bragg–Brentano geometry arrangement using CoKα radiation with a graphite monochromator and a scintillation detector.

Adsorption isotherms of nitrogen at –196 °C were measured with an Accusorb 2100E instrument (Micromeritics). Each sample was degassed at 350 °C for at least 20 h until a pressure of 10^{-4} Pa was attained.

Scanning electron micrographs (SEM) were recorded on an ISI-100B scanning electron microscope operated at 15 kV. Samples were deposited on a sample holder with an adhesive carbon foil and sputtered with gold.

Determination of Material Parameters from Experimental Data

The material parameters of samples prepared were determined as follows. The unit cell constant was calculated according to the formula $a_0 = 2d_{100}/\sqrt{(3)}$, where d_{100} is the interplanar spacing corresponding to the (100) reflection. The total surface area S_{tot}, external surface area S_{ext} and mesopore volume $V_{MCM\text{-}41}$ were determined from nitrogen isotherms by the method of comparison plots[12]. As the surface area S_{ext} includes not only the external surface area of the particles but also the surface area of non-MCM-41 mesopores, the surface area $S_{MCM\text{-}41}$ was calculated by subtracting S_{ext} from S_{tot}. The mesopore diameter $D_{MCM\text{-}41} = 4.20\ V_{MCM\text{-}41}/S_{MCM\text{-}41}$ and pore wall thickness $\Delta = a_0 - 0.95\ D_{MCM\text{-}41}$ were calculated according to formulas based on a geometrical model of the MCM-41 structure[13]. With samples exhibiting the bimodal porous structure, the pore size distribution of non-MCM-41 mesopores was calculated from the desorption branch of the hysteresis loop by the Barrett–Joyner–Halenda method[14]. The total volume of non-MCM-41 mesopores and their mean diameter of selected samples are presented in Table II.

The proportion of silica ordered in the MCM-41 structure was calculated using the formula

$$\%\ \text{of MCM-41 phase} = 100\ V_{MCM\text{-}41} / (V_{MCM\text{-}41})_{pure}\,, \qquad (1)$$

where $V_{MCM\text{-}41}$ and $(V_{MCM\text{-}41})_{pure}$ are the mesopore volume of the sample under study and that of containing exclusively the MCM-41 phase, respectively[8]. As sample 4A is characterized by the highest values of the mesopore volume and surface area, its mesopore volume was used as $(V_{MCM\text{-}41})_{pure}$. The calculated values of the percentage of the MCM-41 phase are given in Table I.

TABLE II
Material parameters of the synthesized silicas

Silica	S_{tot} m^2/g	S_{ext} m^2/g	S_{MCM-41} m^2/g	V_{MCM-41} cm^3/g	D_{MCM-41} nm	Δ nm	a_0 nm	$V_{non-MCM-41}$ cm^3/g	$D_{non-MCM-41}$ nm
1B	98	–	0	0	–	–	–	–	–
4A	1 136	50	1 086	0.866	3.3	1.1	4.38	–	–
5A	1 126	107	1 019	0.790	3.3	1.1	4.42	–	–
5A-S	1 036	123	913	0.716	3.3	1.2	4.54	–	–
9A	961	255	706	0.536	3.2	1.4	4.60	–	–
9B[a]	745	335	410	0.310	~3.2	~1.5	4.69	1.714	~18
9B-S[a]	833	266	567	0.406	~3.0	~1.6	4.56	0.993	~20

S_{tot}, total surface area; S_{ext}, surface area which remains free after filling up the mesopores of the MCM-41 structure; $S_{MCM-41} = S_{tot} - S_{ext}$, V_{MCM-41}, D_{MCM-41}, Δ and a_0, surface area, volume, diameter, pore wall thickness and lattice constant of the MCM-41 structure, respectively.
[a] Samples with a bimodal mesopore structure; $V_{non-MCM-41}$ and $D_{non-MCM-41}$ denote the mesopore volume and mean diameter of the non-MCM-41 mesoporous system.

RESULTS

While sample 1B, prepared without the addition of surfactant, is an X-ray amorphous silica, diffractograms of all other samples proved that they contain some amount of the MCM-41 phase. Three to four reflections were discernible in the range of $2° < 2\theta < 9°$ which can be indexed as (100), (110), (200) and (210) ones assuming the P6 symmetry. Nitrogen isotherm on sample 1B is typical of a non-porous material. Isotherms on samples with a well-developed MCM-41 structure are characterized by a sudden increase in the amount adsorbed in the range of the relative pressure p/p_0 of 0.30–0.35, which is typical of the volume filling of MCM-41 mesopores. Besides, isotherms on some samples display a pronounced hysteresis loop, which reveals the presence of another system of mesopores, whose pore size and volume are much larger. (To avoid possible confusion, it will be in the following denoted as a non-MCM-41 mesopore system.) For this reason, these samples can be identified as a bimodal mesoporous silica.

Synthesis of MCM-41

With the exception of sample 1B, all other samples presented in Table I were prepared at three molar ratios CTABr : $Na_2SiO_3 \approx 0.17$, ≈ 0.33 and ≈ 0.67. In Fig. 1, the corresponding points lie on straight lines *1*, *2* and *3*, respectively. Even though the molar ratio CTABr : $Na_2SiO_3 \approx 0.17$ equals the surfactant content in the as-synthesized MCM-41 (see above), the maximum content of the MCM-41 phase has achieved 80% only. At the molar ratio CTABr : $Na_2SiO_3 \approx 0.33$, the best samples 4A (100% of the ordered phase) and 5A (91%) were prepared, the molar ratio EtAc : Na_2SiO_3 being 1.8 and the water content exceeding 99.7 mole %. When the water content was lower than 99.7% or the ratio EtAc : $Na_2SiO_3 = 3.2$, the amount of the MCM-41 phase decreased. Although the molar ratio CTABr : $Na_2SiO_3 \approx 0.67$ is typical of the preparation of MCM-48 mesoporous molecular sieves[15], no formation of this material was observed. The percentage of the MCM-41 phase ranged from 36 to 72%.

It can be concluded that samples containing over 90% of MCM-41 are formed from reaction mixtures whose compositions are included in the region depicted in Fig. 1 by vertical hatching. The high quality of samples 4A a 5A, corresponding to the extreme limits of the MCM-41 region, is illustrated by X-ray diffractograms and nitrogen isotherms (Figs 2 and 3). The material parameters of these samples are given in Table II.

The SEM image of sample 4A (Fig. 4) prepared from the most dilute reaction mixture shows a regular morphology (particle size of about 1 μm) and a high phase purity. The detailed analysis of particle shapes reveals a well-defined faceting resembling the hexagonal symmetry. Sample 5A, prepared from a less dilute reaction mixture, consists of larger rotational particles (particle size of about 5–6 μm) and contains small proportion of impurities (Fig. 5).

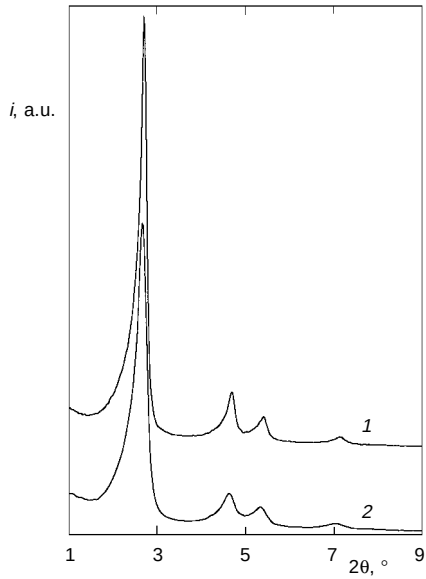

FIG. 2
X-Ray diffraction patterns of silicas 4A (*1*) and 5A (*2*)

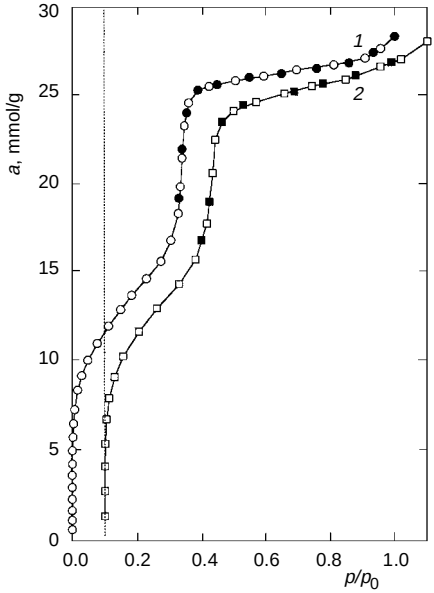

FIG. 3
Adsorption isotherms of nitrogen at –196 °C on silicas 4A (*1*) and 5A (*2*). Solid points denote desorption

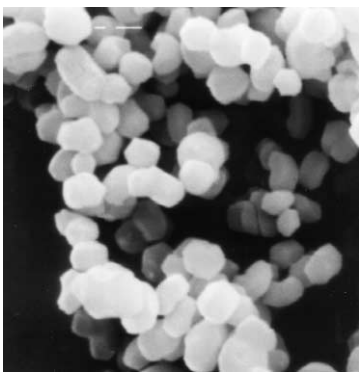

FIG. 4
SEM image of silica 4A. The length of the bar corresponds to 3 μm

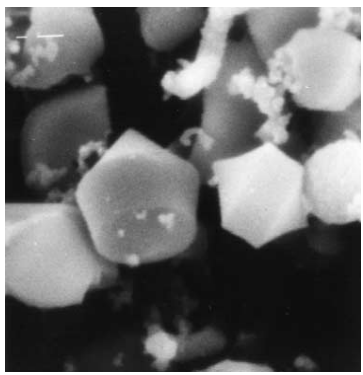

FIG. 5
SEM image of silica 5A. The length of the bar corresponds to 3 μm

Synthesis of Bimodal Silica

In addition to the region of the composition of the reaction mixture corresponding to the MCM-41 material, another one was found which leads to the bimodal silica formed at the ratio EtAc : Na_2SiO_3 = 3.2. This triangular region is depicted in Fig. 1 by horizontal hatching. Figures 6 and 7 show the X-ray diffraction pattern and nitrogen isotherm, respectively, of characteristic sample 9B, which exhibits the largest total volume of both mesopore systems (Table II). The pore size distribution of the non-MCM-41 mesopore system calculated from the desorption branch of the nitrogen isotherm, which is shown in Fig. 8, is relatively narrow with the maximum at the pore diameter of ≈18 nm.

Figure 9 shows the SEM image of sample 9B. This material is characterized by a markedly different morphology in comparison with samples 4A and 5A. Its worm-shaped particles are typical of all samples of bimodal silica prepared under quiescent conditions; its particles are about 1 μm in diameter, their length varying from 10 to 30 μm. The detailed analysis of a number of SEM images has clearly proved that this sample does not contain any impurities.

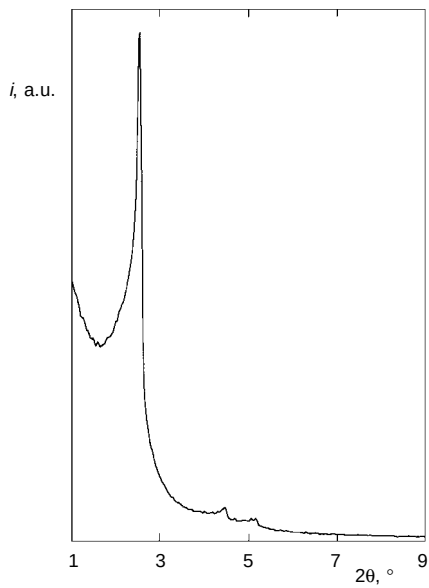

FIG. 6
X-Ray diffraction pattern of silica 9B

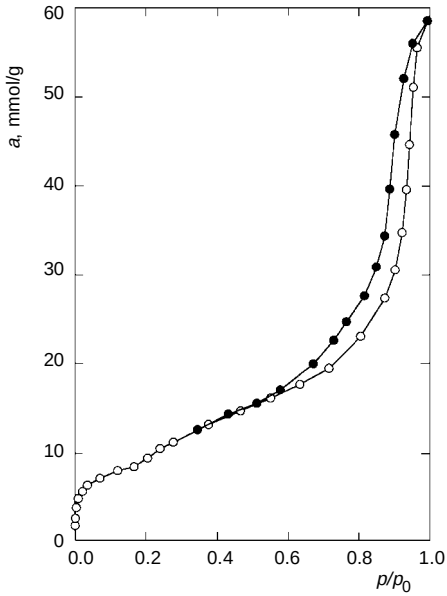

FIG. 7
Adsorption isotherm of nitrogen at –196 °C on silica 9B. Solid points denote desorption

Monitoring pH

In order to investigate the influence of the EtAc content on the precipitation process, the temporal decrease in pH during the ageing of the reaction mixture at ambient temperature under quiescent conditions was monitored. The molar ratio EtAc : Na_2SiO_3 was found to play the key role, *i.e.* at a given value of this ratio, the temporal decrease in pH does not virtually depend on other synthesis parameters. Figure 10 shows a typical time dependence of pH for EtAc : Na_2SiO_3 = 1.8 and 3.2. The larger amount of EtAc obviously causes a much steeper decrease in pH at the beginning of acidification.

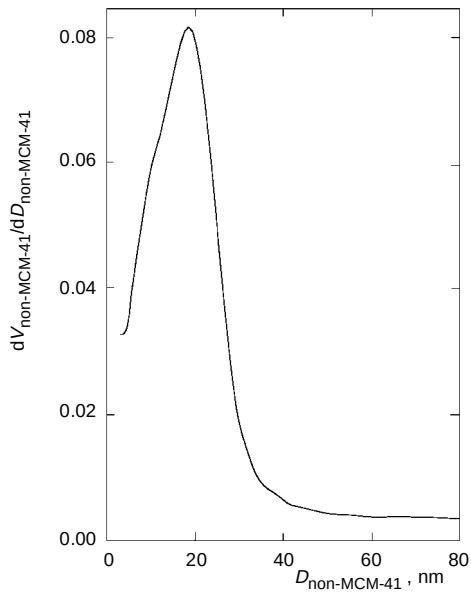

FIG. 8
Pore size distribution of silica 9B

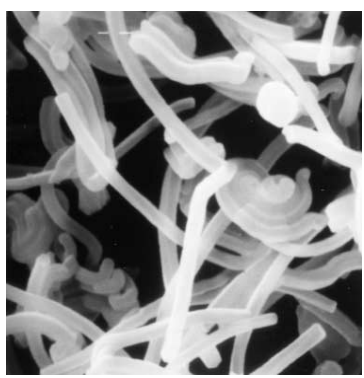

FIG. 9
SEM image of silica 9B. The length of the bar corresponds to 5 μm

Influence of Stirring

The regular morphology of the mentioned materials forms under quiescent conditions only. When stirring was not stopped after the addition of EtAc, a mixture of particles of varying shape and size was formed. A similar effect was also observed by Ozin *et al.*[2]. A comparison of material parameters of samples 5A/5A-S and 9B/9B-S shows that disturbance of the quiescent synthesis slightly influences the proportion of the MCM-41 structure in the materials formed. For example, the content of this structure in sample 5A-S is slightly lower (83%) than that in sample 5A (91%). While the pore volume of the non-MCM-41 porous system of sample 9B-S (bimodal silica) is much lower than that of sample 9B, the proportion of the MCM-41 shows an opposite tendency.

Reproducibility

Analogously to the determination of the percentage of silica ordered in the MCM-41 structure, the mesopore volumes $V_{\text{MCM-41}}$ and $V_{\text{non-MCM-41}}$ (see Table II) can be taken as a measure of the proportion of corresponding mesoporous structures. The value of $V_{\text{MCM-41}}$ of sample 5A repeatedly synthesized from batches of different size (starting amounts of Na_2SiO_3 varying between 5–25 g) but with the same composition has been found to vary within a very narrow range between 0.785 and 0.790 cm^3/g. The analogous experiments with sample 9B has provided the same results, $V_{\text{MCM-41}}$ ranging be-

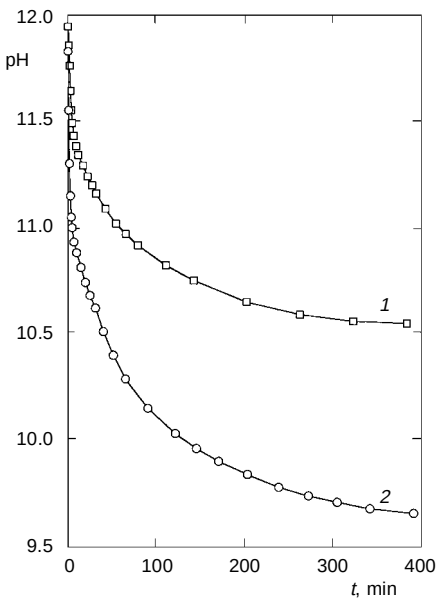

FIG. 10
Time dependence of pH of the reaction mixture for the EtAc : Na_2SiO_3 molar ratios 1.8 (*1*) and 3.2 (*2*)

tween 0.300 and 0.310 cm^3/g and $V_{non\text{-}MCM\text{-}41}$ between 1.681 and 1.714 cm^3/g. Therefore, the reproducibility of the synthesis procedure can be regarded as excellent.

DISCUSSION

A study of the dependence of pore structure parameters, particle morphology and phase purity on the composition of the reaction mixture under quiescent conditions has shown that the formation of well-defined materials proceeds in two regions of the synthesis field only. This rather restricting condition, on the other hand, makes possible to suggest a mechanism which controls the formation of the mesopore structure and the particle morphogenesis. To this end, the results published in the literature obtained using specialized experimental methods, such as cryo-transmission electron microscopy[16], will be also used to support the presented mechanism.

The isotropic solution of the reaction mixture before the beginning of acidification contains disordered elongated rod-like micelles, whose surface is partly covered by silicate anions. These anions replace the original bromide counteranions due to their lower degree of dissociation (approximately 25% and less than 7% with Br^- and double- or polycharged silicate anions, respectively[17]). Due to the degree of dissociation mentioned, the surface of micelles is partly covered with silicate anions. The binding of silicate anions to the positively charged headgroups reduces the charge density of the micelle surface much more effectively than bromide counteranions. In this way, all transformations of the shape of micelles (such as the sphere-to-rod transition) are induced at much lower surfactant concentrations and also the mean micellar aggregation number is increased[18].

Precipitation at the EtAc : Na_2SiO_3 Molar Ratio 1.8

Owing to the decrease in pH due to the hydrolysis of EtAc, silicate anions in the reaction mixture begin to polymerize. This polymerization comprises three processes, which proceed simultaneously. First, silicate anions bound to the surface of micelles polymerize to form polyanions (intramicellar polymerization). Second, micelles partly covered by silicate polyanions are gradually arranged into a hexagonal array through the intermicellar silicate condensation. (The terms intramicellar and intermicellar polymerization were introduced in ref.[18].) Free silicate anions or polyanions provide further building material for the formation of the silica walls between the micelles. Finally, at a sufficiently high concentration, caused by an inappropriately selected composition of the reaction mixture, free silicate anions/polyanions can polymerize to form amorphous silica.

Pure MCM-41 (sample 4A) was prepared from the reaction mixture with molar ratio CTABr : $Na_2SiO_3 \approx 0.33$. This ratio corresponds to that determined by Klinowski *et al.*[19] as optimum for the synthesis of MCM-41. At molar ratios CTABr : Na_2SiO_3 lower than

the optimum (*e.g.* ≈0.17), an excess of free silicate anions in the reaction mixture (anions not bound to the surfactant micelles) clearly polymerizes to form amorphous silica. On the other hand, at molar ratios CTABr : Na_2SiO_3 larger than the optimum (*e.g.* ≈0.67), the decreased amount of free silicate anions in the reaction mixture is clearly insufficient for the formation of stable silica walls between micelles.

Material properties of samples 4A and 5A show that the dilution of the reaction mixture determines the porous structure and morphology of solid particles. Sample 4A is a pure MCM-41 with regular morphology; therefore, in a highly dilute reaction mixture, the polymerization of silicate anions occurs preferentially *via* the intramicellar and intermicellar condensation. The very low concentration of free silicate anions prevents the formation of amorphous silica. It can be assumed that the shape of particles of sample 4A (Fig. 4) reflects the highly regular internal structure. As the molar ratio CTABr : Na_2SiO_3 ≈ 0.33 of the corresponding reaction mixture is virtually twice as large as that of an as-synthesized MCM-41 material, a certain proportion of silicate anions or polyanions, which participate in the process of the formation of MCM-41 walls, originates from micelles which have not been built in the MCM-41 structure. Silicate anions have been released from the surface of these micelles by dissociation and ion-exchanged mainly for bromide anions. Finally, it should be mentioned that approximately hexagonal, faceted particles were obtained by Beck *et al.*[2] as early as 1992. Their particles, however, were substantially smaller (0.05–0.2 μm) and did not constitute majority in a mixture of variously shaped particles, *i.e.*, the product was far from uniform.

Sample 5A was prepared from a less dilute reaction mixture. (The concentrations of Na_2SiO_3 and CTABr are approximately by one order higher than those in sample 4A.) Therefore, the growth of its particles was faster and their size larger. The higher concentration of free silicate anions caused that some amount of amorphous silica has formed, which is apparent from a slightly smaller percentage of the MCM-41 phase in comparison with sample 4A (Table I). The rotational particle shape of sample 5A is similar to that observed by Ozin *et al.*[6,20,21] who have suggested an explanation based on stresses induced by the polymerization of silicate species between micelles. This explanation is supported by a decrease in the intermicellar distance which has been observed at the early stages of the synthesis[22].

Precipitation at the EtAc : Na_2SiO_3 Molar Ratio 3.2

As the percentage of MCM-41 phase of the samples prepared at the EtAc : Na_2SiO_3 molar ratio 3.2 does not exceed 48%, the higher rate of acidification of the reaction mixture is clearly unfavourable for the formation of this structure and leads to the formation of bimodal silica.

Sample 1B, prepared under the same conditions as those of sample 9B of bimodal silica but in the absence of surfactant (Table I), has a non-porous structure. Conse-

quently, the non-MCM-41 mesoporous system cannot be formed without the action of CTABr as a structure-directing agent. A study of the early stages of the formation of silica walls between micelles, using sophisticated experimental methods, has shown that clusters of rod-like micelles are "wrapped" with a silicate film which, in the course of reaction, penetrates them[16]. It can be expected that the mentioned silicate film "freezes", due to the fast polymerization caused by the higher rate of acidification, before it can penetrate micelle clusters; thus, the non-MCM-41 mesoporous system is templated by them. This explanation is supported by the fact that all samples of bimodal silica were prepared from relatively concentrated reaction mixtures. Therefore, the probability of formation of micelle clusters was higher than that with more dilute reaction mixtures used for preparation of pure MCM-41.

The worm-shaped morphology of bimodal silica is most probably formed by the mechanism of "end effects" of cylindrical micelles. As shown by Ozin *et al.*[21], the surfactant micelles (and, consequently, also the mesopores) run continuously throughout the body of the micrometer dimension mesoporous silica particles. In our opinion, the formation of long micelles running throughout the particles is a general phenomenon. At each end of a cylindrical micelle, the surfactant molecules are forced to pack into hemispherical caps; the headgroup area of the surfactant molecules forming the caps is approximately 1.5 times larger than that of the surfactant molecules assembled in the cylindrical part of the micelle. The energetically unfavourable packing of the surfactant molecules in the caps may be eliminated if the ends of the two micelles link[23]. This fact, together with the lower density of anions which cover the caps of micelles (given by the larger headgroup area of the surfactant molecules), can be expected to be the cause of linking the micelles in the direction of their longitudinal axes. The relatively high concentration of the reaction mixture produces favourable conditions for the growth of the evolving worm-shaped particles. The proposed mechanism of the growth of bimodal silica particles is also supported by transmission electron microscopy images published by Ozin *et al.* and their idea that the deposition process is favoured at the sticky surfactant-silicate ends of long cylindrical particles[6].

CONCLUSIONS

The developed procedure for synthesis of siliceous mesoporous materials is advantageous for the following reasons: First, it is excellently reproducible and leads to materials with regular morphologies. Second, it enables obtaining not only siliceous MCM-41 molecular sieves with the highest degree of pore ordering, regular morphology and phase purity but also a material of a new type, *viz.* bimodal silica.

Bimodal silica contains both the MCM-41 mesopore system and the system of larger mesopores whose size ranges from 15 to 25 nm. The total surface area of bimodal silica attains ≈750 m^2/g, the total mesopore volume ≈2 cm^3/g. Owing to these structural properties, the bimodal silica is comparable with silica aerogels[24] and can be a promi-

sing material for applications in separation processes or as a support for bulky molecules or nanoparticles.

A research grant from the Volkswagen Foundation (grant No. I/72134) is gratefully acknowledged. We thank Ms A. Toltz (University of Bremen, FB 2, UFT) for recording SEM images.

REFERENCES

1. Kresge C. T., Leonowicz M. E., Roth W. J., Vartuli J. C., Beck J. S.: *Nature* **1992**, *359*, 710.
2. Beck J. S., Vartuli J. C., Roth W. J., Leonowicz M. E., Kresge C. T., Schmitt K. D., Chu C. T.-W., Olson D. H., Scheppard E. W., McCullen S. B., Higgins J. B., Schlenker J. L.: *J. Am. Chem. Soc.* **1992**, *114*, 10834.
3. Sayari A.: *Stud. Surf. Sci. Catal.* **1996**, *102*, 1.
4. Corma A.: *Chem. Rev.* **1997**, *97*, 2373.
5. Rathousky J., Zukalova M., Zukal A.: *Collect. Czech. Chem. Commun.* **1998**, *63*, 271.
6. Hong Yang, Coombs N., Ozin G. A.: *Nature* **1997**, *386*, 692.
7. Grun M., Lauer I., Unger K. K.: *Adv. Mater.* **1997**, *9*, 254.
8. Schulz-Ekloff G., Rathousky J., Zukal A.: *Microporous Mesoporous Mater.*, in press.
9. Khushalani D., Kuperman A., Ozin G. A., Tanaka K., Garces J., Olken M. M., Coombs N.: *Adv. Mater.* **1995**, *7*, 842.
10. Chen C.-Y., Li H.-X., Davis M. E.: *Microporous Mater.* **1993**, *2*, 17.
11. Romero A. A., Alba M. D., Zhou W., Klinowski J.: *J. Phys. Chem. B* **1997**, *101*, 5294.
12. Rathousky J., Schulz-Ekloff G., Zukal A.: *Microporous Mater.* **1996**, *6*, 385.
13. Schulz-Ekloff G., Rathousky J., Zukal A. in: *Synthesis of Porous Materials*, (M. L. Occelli and H. Kessler, Eds), p. 391. Dekker, New York 1997.
14. Barrett E. P., Joyner L. G., Halenda P. P.: *J. Am. Chem. Soc.* **1951**, *73*, 373.
15. Schmidt R., Stocker M., Akporiaye D., Torstad E. H., Olsen A.: *Microporous Mater.* **1995**, *5*, 1.
16. Regev O.: *Langmuir* **1996**, *12*, 4940.
17. Huo Q., Margolese D. I., Ciesla U., Demuth D. G., Feng P., Gier T. E., Sieger P., Firouzi A., Chmelka B. F., Schuth F., Stucky G. D.: *Chem. Mater.* **1994**, *6*, 1176.
18. Lee Y. S., Surjadi D., Rathman J. F.: *Langmuir* **1996**, *12*, 6202.
19. Cheng C.-F, Park D. H., Klinowski J.: *J. Chem. Soc., Faraday Trans.* **1997**, *93*, 193.
20. Ozin G. A., Hong Yang, Sokolov I., Coombs N.: *Adv. Mater.* **1997**, *9*, 662.
21. Coombs N., Khushalani D., Oliver S., Ozin G. A., Guo Cheng Shen, Sokolov I., Hong Yang: *J. Chem. Soc., Dalton Trans.* **1997**, 3941.
22. Rathousky J., Zukal A., Had J.: Unpublished results.
23. Israelachvili J. N.: *Intermolecular and Surface Forces*, p. 374. Academic Press, New York 1992.
24. Husing N., Schubert U.: *Angew. Chem., Int. Ed. Engl.* **1998**, *37*, 23.